Noise studies with Crab Cavities in the SPS for the HL-LHC project

Thesis submitted in accordance with the requirements of the University of Liverpool for the degree of Doctor in Philosophy

by

Natalia Triantafyllou

Day Month Year

Abstract

Acknowledgments

List of Figures

List of Tables

List of Symbols

E_b Energy

CC   Crab Cavity

V_{CC} CC voltage

f_{CC} CC frequency

ϕ_{CC} CC phase

Q_x Horizontal tune

Q_y Vertical tune

ψ_y Vetical phase advance

β Relativistic beta

γ Relativistic gamma (Lorenz factor)

Contents

1 | Introduction

This is the introduction of my PhD thesis.

In 2018, two prototype Crab Cavities (CCs) were installed in the SPS to be tested for the first time with proton beams. A series of dedicated machine developemnt studies was carried out in order to validate their working principle and answer various beam dynamic questions. One of the operational issues that needed to be addressed concerned the expected emittance growth due to noise in their RF system, which is the main subject this thesis. As mentioned in chapter 3 a theoretical model had already been developed and validated by trackig simulations [1]. As a part of the first experiemental campaign with CCs in SPS a dedicated experiment was conducted to benchmark these models with experimental data and confirm the analytical predictions. The objective of this chapter is to provide an overview of the machine setup for the CC experiements and introduce the instruments and methods used for measuring the beam parameters of interest for the emittance growth studies.

2 | Basics of accelerator beam dynamics

For a gaussian beam distribution the normalised beam emittance is defined as:

$$\epsilon_x = \frac{\sigma_x(s)^2 - \delta^2 D_x^2(s)}{\beta_x(s)} \beta\gamma \tag{2.1}$$

where $\sigma_x(s)$ is the beam size, $\beta_x(s)$ is the beta function, $D_x(s)$ is the dispersion fat a specific location s along the accelerator, $\delta = \Delta p/p0$ is the momentum spread and β, γ the relativistic parameters. Similar expression is valid for the vertical plane, with the difference that there is no dispersion.

3 | Theory of Crab Cavity noise induced emittance growth

4 | Experimental studies 2018: Operational setup and beam instrumentation

The theoretical model for the transverse emittance growth caused by amplitude and phase noise in a CC was introduced in Chapter 3. In 2018, a dedicated experiment was conducted in the SPS to benchmark these models with experimental data and confirm the analytical predictions. Here, the objective is to provide an overview of the machine setup and the beam instrumentation used for the emittance growth studies with CCs in the SPS.

The chapter is structured as follows: Section 4.1 describes the experimental machine configuration. Thereafter, Section 4.2 elaborates on the installation and the operation of the CCs in the SPS. In Sections 4.3- 4.6 the instruments used for the parameters of interest (see Chapter 3, Eq....) i.e. CC voltage, emittance and bunch length are discussed, including the post processing methods where it was performed by myself.

4.1 Machine configuration

In view of the CCs operation in HL-LHC where the beam will stay in the machine for sevral hours, special cycles were setup in the SPS for the emittance growth studies with CCs. They are called "coast" bunched beam cycles and during them the bunches circulate in the machine at constant energy for long periods up to a few hours.

As the project of the CCs aims to the LHC were the beam stays in the machine for hours. Thus, for the emittance growth studies with CCs in the SPS special cycle was

setup, which are called "coast" bunched beam cycles. This term

a special machine configuration was set up called 'coast' beam cycles with bunched beam. Long time conservative

The available time for testing the CC noise induced emittance growth was very limited. Therefore, a number of thorogh preparatory have been performed in advance Ref[...]

One of the major concerns was the natural emittance growth observed in SPS in coast. The reason is not yet well understood. However, it was identified that is minimum for higher energies. Now the higher energy that the SPS can operate in coast is 270 GeV. Thus, the emittance growth experiemtns were performed at 270 GeV

A number of preparatory studies have been perforemd the years before 2018, in order to define the optimal machine configuration for the experimental study of the CC noise induced emittance growth.

- Energy - chromaticity. Dependence of natural emittance growth to chromaticity. It was kept minimum. Measurements not available but we will consider small value 1.
- To simplify the study the octupoles were switched OFF. For the model to apply we need a tune spread from amplitude detuning. THe octupoles were switched off as the resitudal non lineariteis Ref to micheles paper result to a sufficient tune spread of 10^-4.

4.2   Crab Cavities in the SPS

For the SPS tests two prototype CCs of the Double Quorter Wave (DQW) type were fabricated by CERN and were assembled into the same cryomodule which is shown in Fig. 4.1 [2]. The cryomodule was installed in the SPS-LSS6 zone, Fig. 4.2, and was placed on a mobile transfer table [3]. The table moved with high precision and without breaking the vaccum the cryomodule in the beam line for the CC tests and out of it for the usual SPS operation. The main parameters for the CC experiments in SPS are shown in Table 4.1
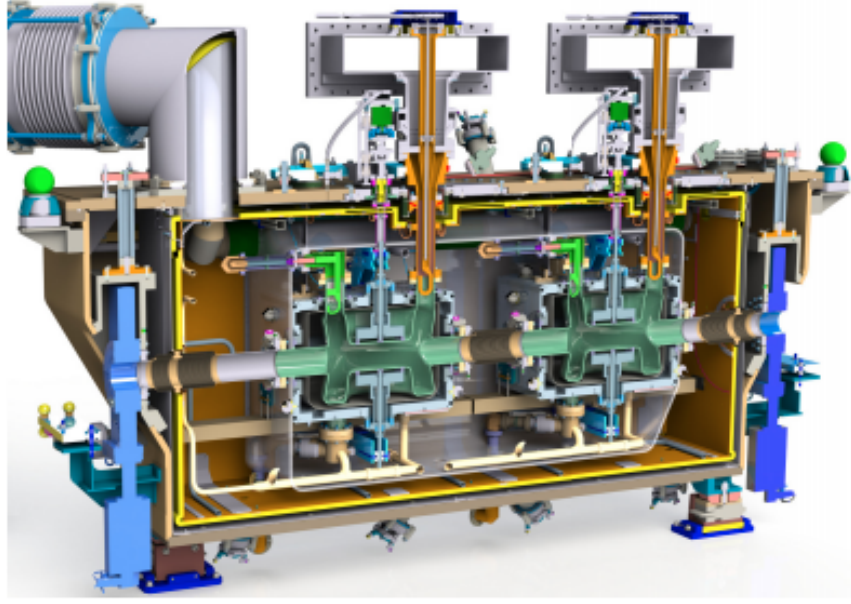
Figure 4.1: Cut of the CC cryomodule [2].

Table 4.1: Main parameters for the emittance growth studies with CCs in SPS in 2018

Parameters	Units	Values	
E_b	[GeV]	26, 270	
Main RF frequency	[MHz]	200	
Q_x / Q_y	[-]	26.13 / 26.18	
		CC1	**CC2**
crabbing plane	[-]	vertical	vertical
s-location	[m]	6312.72	6313.32
V_{CC}	[MV]	0	1
f_{CC}	[MHz]	400	400
$\beta_{x,CC}$ / $\beta_{y,CC}$	[m]	29.24 / 76.07	30.31 / 73.82
$\alpha_{x,CC}$ / $\alpha_{y,CC}$	[m]	-0.88 / 1.9	-0.91 / 1.86
$D_{x,CC}$ / $D_{y,CC}$	[m]	-0.48 / 0	-0.5 / 0

4.2.1 Operational considerations

For the beam tests with the CCs in the SPS the approach regarding the energy ramp

and the adjustment of the phasing with the main RF system needed to be evaluated
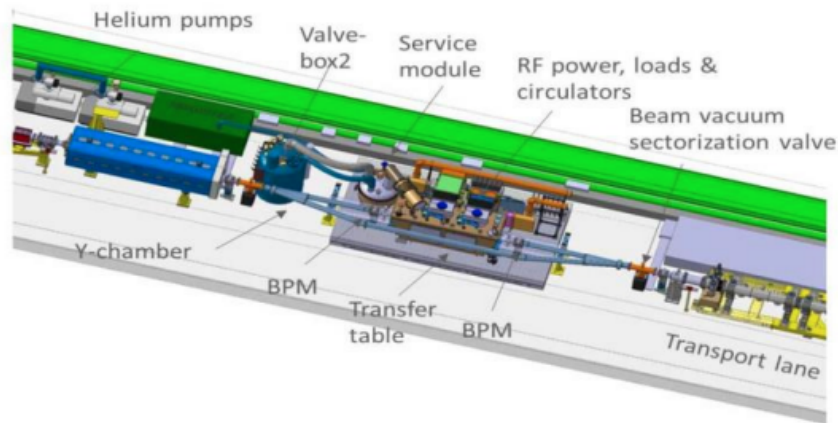
Figure 4.2: Installation of the cryomodule in the SPS-LSS6 zone [3].

and they are briefly discussed here.

Energy ramp

SPS recieves the beam at 26 GeV. It was observed that if the ramp to higher energies was performed with the CC on, the beam was lost while crossing one of the vertical betatron sidebands due to resonant excitation [4]. Therefore, it was established that the acceleration has to be performed with the CC off and its voltage must be set up only after the energy of interest has been achieved. It should be noted here that this will be the approach also for the HL-LHC.

Crab Cavity - main RF synchronisation

Another issue of concern was the fact that the CC operate at the fixed frequency of 400 MHz while the SPS main RF system operates at 200 MHz. In order to make sure that the beam will experience the same effect from the CC each turn the SPS main RF has to be re-phased such as it becomes synchronous with the crabbing signal. For studies at the injection energy of 26 GeV this synchronisation took place shortly after the injection. For studies at 270 GeV, like the emittance growth measurements, the synchronisation took place at the end of the ramp shortly after the cavity was switched on [5].

8

4.3 SPS Head-Tail monitor

The HT monitor was the main diagnostic device deployed for the callibration of the CC voltage. Additionally, it was used for the measurement and the physical illustration of the crabbing. This made it a very useful tool in the time of the experiments as it provided a direct validation of the effect of the CC kick on the beam. The HT monitor was originally designed for measuring chromaticity and transverse isntabilities. Therefore its use as a crabbing diagnostic should be explained here. The methods and procedures described in this section were developed at CERN and they are described here for the completness of the thesis.

In the first part of this section some general information on the instrument along with example signals will be presented. Subsequently, the post processing of the HT signal in the presence of the CCs. Last, the callibration of the CC voltage from the HT data is described. The experiemental data presented in this section were acquired at the SPS injection energy of 26 GeV with only one CC, CC1, at $\phi_{CC} = 0$ for simplicity. That energy option was chosen as the effect of CC kick on the beam is stronger and thus more visible than in higher energies.

General information

The HT monitor is a high bandwidth version of a standard beam position monitor

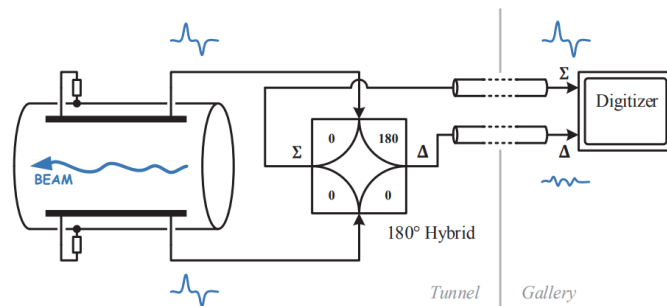Figure 4.3: Diagram of the SPS HT monitor [6].

but it can measure the transverse offset within the bunch. This makes it ideal for the measurement of the intra-bunch offset caused from the CC kick. Its reading consists of the sum Σ and the difference Δ of the electrode signals of a straight stripline coupler (Fig. 4.3) [7, 6] over a defined acquisition period. The Σ signal is the longitudinal

line density while the Δ signal corresponds to the intra-bunch offset.

The raw signals from the HT monitor require a specific post processing procedure, which is described in Ref. [6], in order to give useful information. Figure 4.4 shows some example signals obtained from the HT monitor after the basic post procesing is applied. Moreover, Fig. 4.5 shows a 2D representation of the HT monitor reading. It is worth noting here that in the specific example a clear periodic oscillation of the vertical intra-bunch offset (vertical Δ) signal is observed. This is a result of the main RF system not being synchronous with the CC frequency.
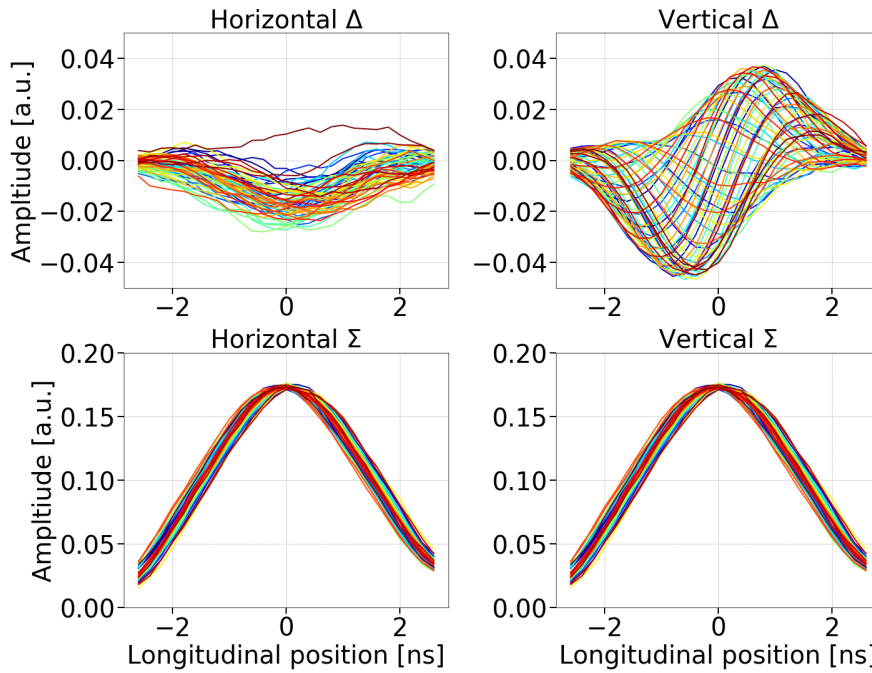
Figure 4.4: Example Δ and Σ signals from the HT monitor with respect to the longitudinal position within the bunch over several SPS revolutions, after the basic post processing (Ref. [6]) but before the baseline correction. The different colors indicate the signals from different turns.

4.3.1   Post processing in the presence of Crab Cavities

To obtain useful information from the HT monitor signal in the presence of the CCs there are a few steps that differ from the standard post processing procedure and they are desribed below.

Heat-Tail monitor baseline correction

One issue of concern is the correction of the Δ signal baseline due to orbit offsets
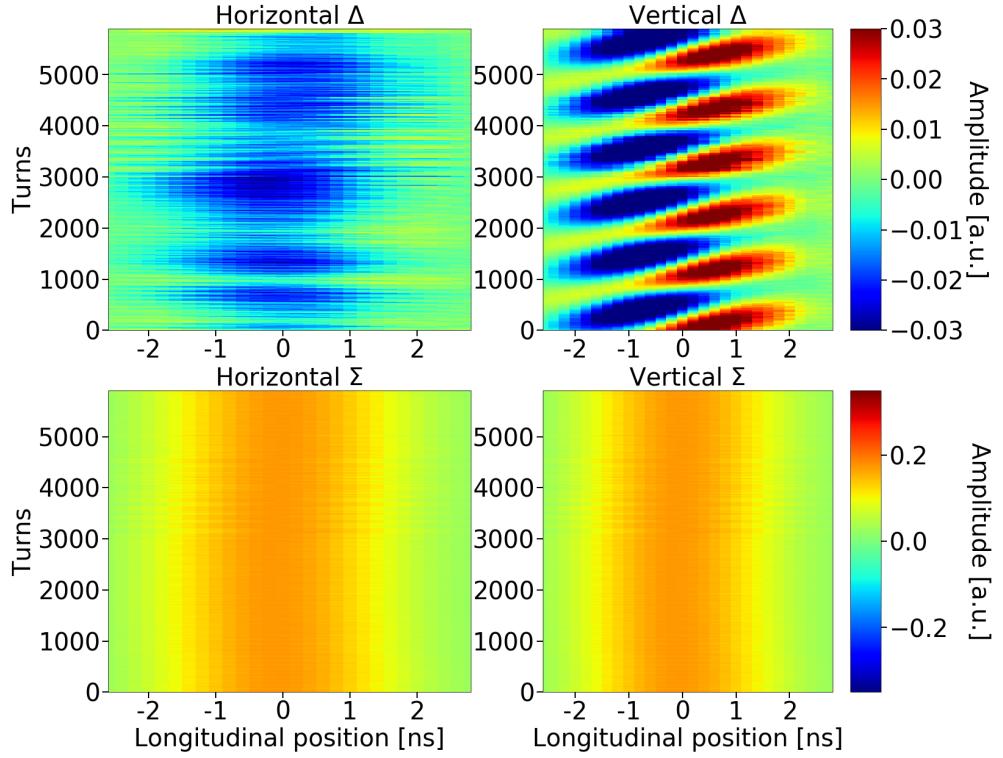
Figure 4.5: 2D representation of example Δ and Σ signals with respect to the longitudinal position within the bunch obtained from the HT monitor over several SPS revolutions.

and non-linearities of the instrument [6]. During the normal post processing, the correction is achieved by computing the mean of the Δ signals over all turns and then subtracting this static offset from the signal of each turn. However, in the SPS tests, where the CCs are well synchronised with the main RF system (Section 4.2), the crabbing signal is also a static intra-bunch position offset and thus would also be removed with the usual method.

Therefore, for the CC experiments a reference measurement had first to be made with the CC unsynchronised. The mean of the Δ signal over this reference period was the baseline which then was subtracted from the Δ signals acquired after the synchronisation (Fig 4.6). The datasets before and after synchronisation are easily distinguishable in the 2D HT monitor reading as displayed in Fig. 4.7

Headtail monitor callibration

The last step, to make the HT acquisitions meaningful is to convert the measured intra bunch offset, $\langle\Delta\rangle$, from arbitrary units to mm. The scaling is achieved by di-
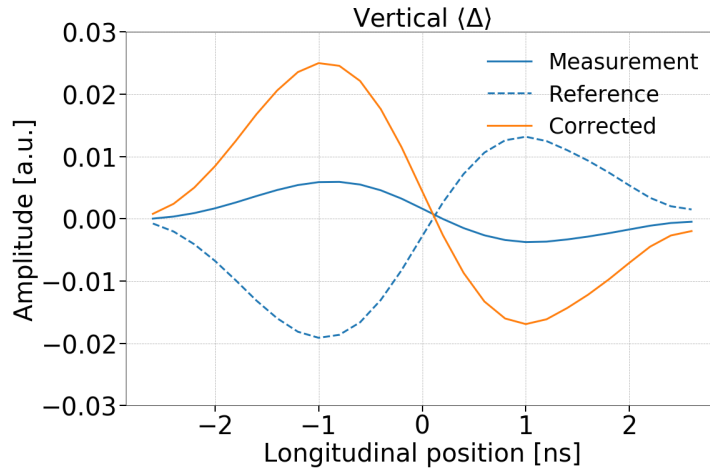
Figure 4.6: HT monitor baseline correction for the SPS CC tests.
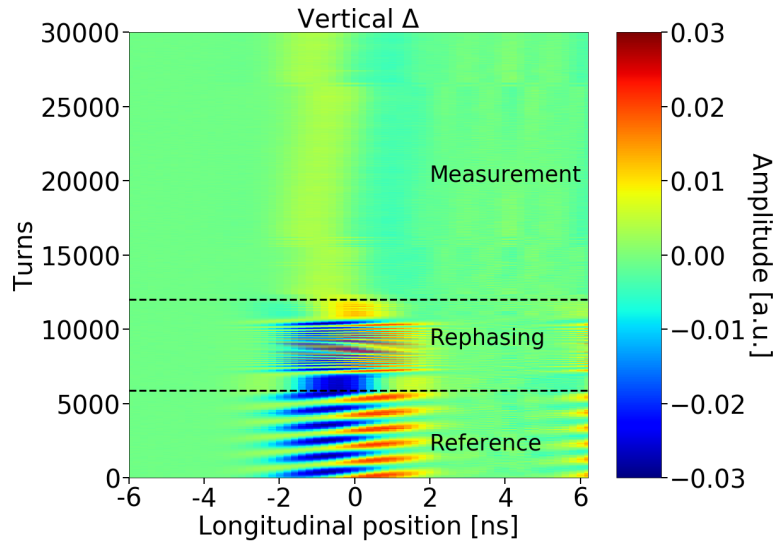
Figure 4.7: HT acquistions before and after the sunchronisation of the SPS main RF with the CC.

vision with the $\langle \Sigma \rangle$ signal and with a normalisation factor which is provided by the calibration of the HT monitor [8]. The normalisation factor for the SPS was measured at 0.1052 in 2018 [9]. Figure 4.8 shows the intra bunch offset from the CC kick in mm and after the baseline correction.

4.3.2 Crab Cavity voltage calibration

This section discusses the beam based measurement of the CC voltage from the HT monitor signal. The calibration was performed by calculating the kick required to reconstruct the measured intra-bunch offset using Eq. (4.1). Equation (4.1), which
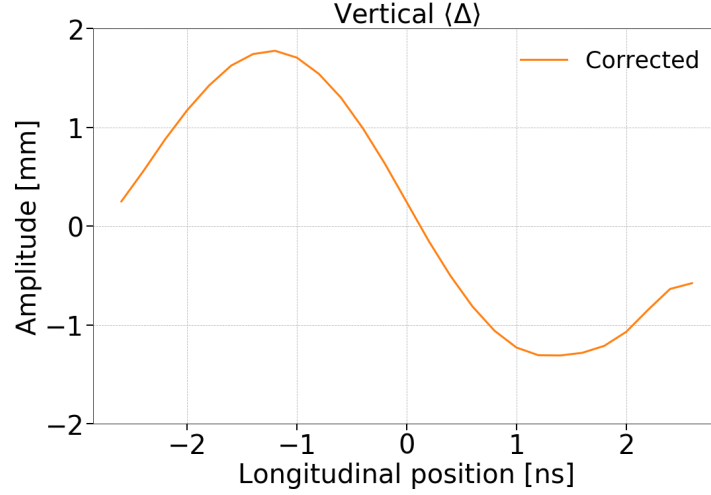
Figure 4.8: Intra-bunch offset from the CC kick expressed in mm after the removal of the baseline.

is obtained from Chaos' Eq. (1) from chapter 4.7.1 in Ref. [10], gives the vertical orbit shift (in meters) from the CC kick, θ, at the HT monitor location as follows:

$$\Delta y_{,HT} = \frac{\sqrt{\beta_{y,HT}}}{2\sin(\pi Q_y)}\theta\sqrt{\beta_{y,CC}}\cos(\pi Q_y - |\psi_{y,HT} - \psi_{y,CC}|),\qquad(4.1)$$

where β_y is the beta function, Q_y is the tune, and ψ_y is the phase advance in tune units. The same applies for the horizontal plane. The indeces HT and CC indicate the optic parameters at the location of the HT monitor and CC respectively.

The deflection from the CC is written as $\theta = -\frac{qV(t)}{E_b}$, where q is the charge of the particle, E_b the beam energy and $V_{CC}(t) = V_{CC}\sin(2\pi f_{CC}t + \phi_{CC})$ is the voltage that a particle experiences while passing through the CC. Computing the maximum of $V_{CC}(t)$ gives the cavity voltage, V_{CC}.

It should be noted here, that the measured intra-bunch offset, $\Delta y_{,HT}$, is inserted in Eq. (4.1) after removing the baseline and converting it in mm as discussed in Section 4.3.1. Figure 4.9 illustrates the cavity voltage computed from the HT signals shown already in this section. The corresponding beam and optic parameters are listed in Table 4.2

Reconstruction of crabbing

The reconstruction of the crabbing from the HT monitor measurements and the
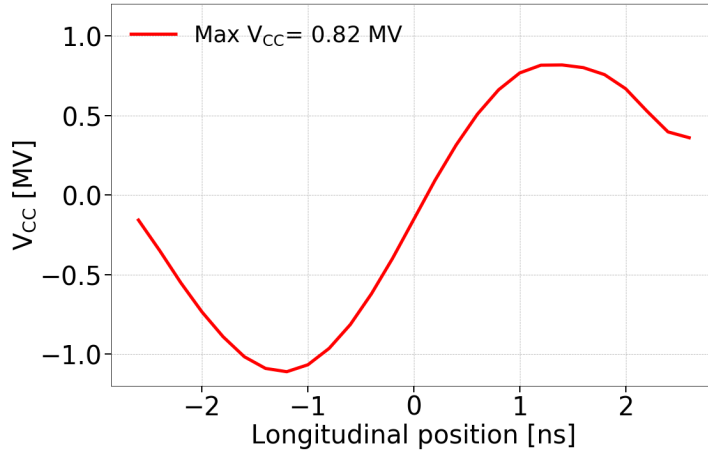
Figure 4.9: CC voltage calibration from the HT monitor.

Table 4.2: Parameters for computing the CC voltage from the example HT monitor measurements discussed in this chapter

Parameters	Units	Values
$\beta_{y,HT}$ / $\beta_{y,CC1}$	[m]	49.19 / 76.07
$\psi_{y,HT}$ / $\psi_{y,CC1}$	[-]	15.68 / 23.9
Q_y	[-]	26.13
E_b	[GeV]	26

physical illustration of it are paresented here. This technique was developed at CERN in 2018 and it was extensivley used throught the experimental campaign with CCs as alongside the calibrated voltage it gives a straightforward estimation of the applied CC kick, as illustrated in Fig. 4.10.

To obtain this physical illustration of the effect of the CC kick on the beam one needs to modualte the measured longitudinal profile, $\langle\Sigma\rangle$, with the measured intra-bunch offset (e.g. Fig. 4.8). For the transverse plane a gaussian distribution is considered with σ obtained from the wire scanner (addressed in more details in the following section). The color code is normalised to the maximum intensity within the bunch.
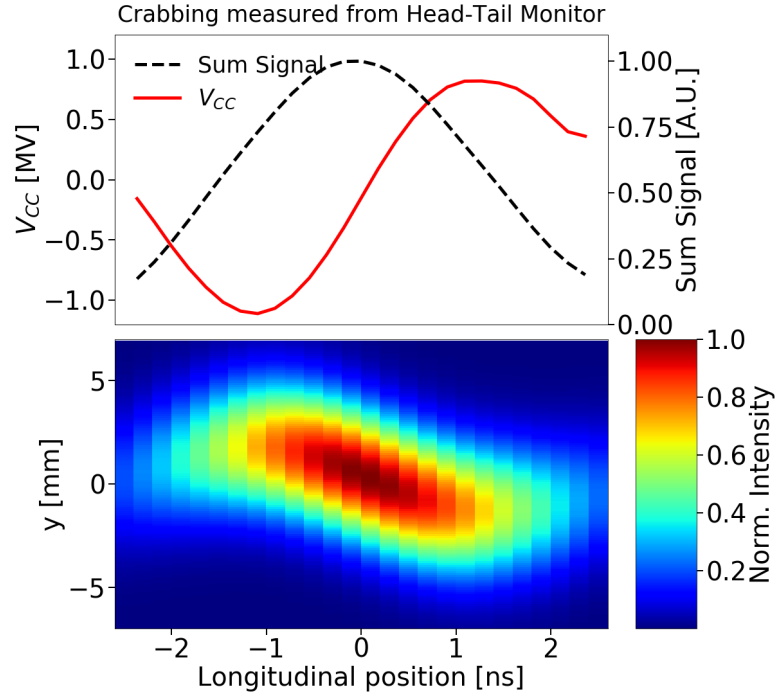
Figure 4.10: Illustration of the crabbing from the HT monitor signal.

4.4 SPS Wire Scanners

The SPS is equpped with beam wire scanners (WS) to measure the transverse beam emittance. The SPS WS system is described in detail in Ref. [11, 12]. For the SPS tests, the emittance was measured with rotational WS both for the horizontal and vertical plane (BWS.51995.H and BWS.41677.V respectively).

The working principle is shown in Fig. 4.11. A thin wire rapidly moves across the proton beam and a shower of secondary particles is generated. Their signal is then detected by a system of scintillator/photomultiplier (PM) outside of the beam pipe. By measuring the wire position and the PM current at it over multiple turns the transverse beam profile is reconstructed. An example of a vertical profile is shown in Fig. 4.12 (left).

Fitting of transverse profiles

To obtain the beam size, σ, the transvserse profiles from each scan are fitted with a four parameter Gauss function:

$$f(x) = k + Ae^{-\frac{(x-\mu)^2}{2\sigma^2}},$$
(4.2)

15

Figure 4.11: Sketch of the SPS rotational wire scanners [12]

where k is the signal offset of the PM, A is the signal amplitude, μ is the mean of the Gaussian distribution and $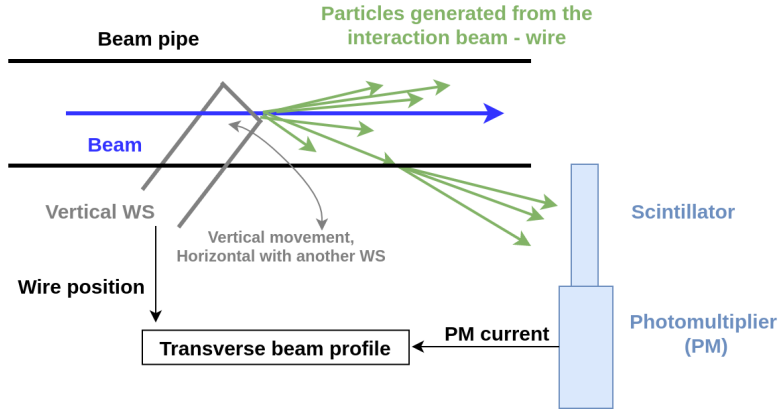\sigma$ its standard deviation. The uncertainty of the measured beam size, $\Delta\sigma$, is defined as the one standard deviation error on σ which is computed from the square root of the diagonal elements of the covariant matrix.
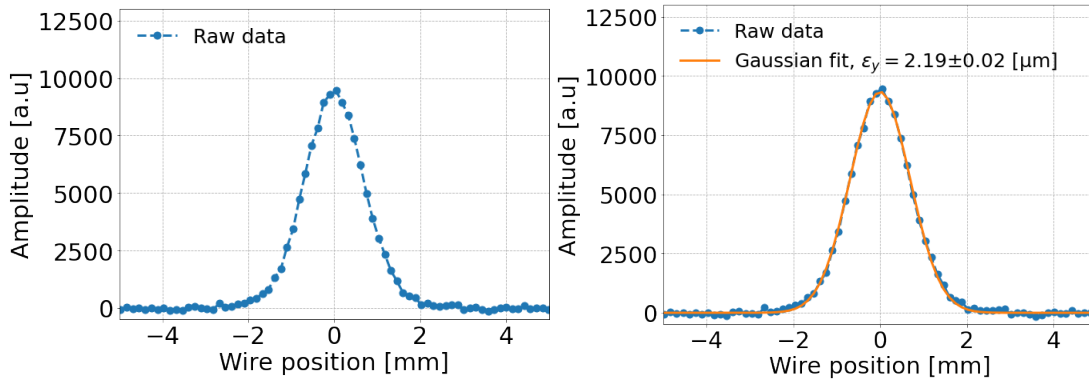
Figure 4.12: Vertical beam profile obtained from the BWS.41677.V instrument. The measuremed data points (light blue) are fitted with a four parameter Gaussian (orange) to obtain the beam size. The calculated emittance is also shown.

The general formula for computing the normalised beam emittance from the beam size, σ is described in Eq. (2.1). However, in the 2018 SPS operational configuration, the dispersion was small in the WSs location and thus its contribution to the beam size was considered to be negligible [1]. In that case, the normalised emittance can be

---

[1]The dispersion at BWS.51995.H location in 2018 was D_x = -15 mm. At 270 GeV, δ is of the order of 10^{-4}. Thus, from Eq. (2.1) the horizontal normalised emittance from the dispersion is foreseen at the order of 10^{-11}. Comparing to the observed beam size during the CC tests of a few microns the

16

calculated for both transverse planes simply from the beam size (σ), the beta function at the WS location (β_{WS}), and the relativistic parameters (β, γ) as follows:

$$\epsilon = \frac{\sigma^2}{\beta_{WS}} \beta\gamma \tag{4.3}$$

The beta functions were 81.5 m and 62.96 m at the locations of the horizontal and vertical WS respectively.

Considering that the relativistic parameters and the beta fucntion are free of error, the uncertainty of the computed emittance, $\Delta\epsilon$, at a dispersion free region, depends only on the uncertainty of the measured beam size, $\Delta\sigma$, as:

$$\frac{\Delta\epsilon}{\epsilon} = \sqrt{\left(2\frac{\Delta\sigma}{\sigma}\right)^2} = 2\frac{\Delta\sigma}{\sigma}, \tag{4.4}$$

Further considerations

It is worth noting here, that during each measurement with the WS the beam profile is actually acquired twice as the wire crosses the beam at the forward direction (IN scan) and then backwords (OUT scan). For the 2018 measurements the emittance values obtained from IN and OUT scans, $\epsilon_{IN} \pm \Delta\epsilon_{IN}$ and $\epsilon_{OUT} \pm \Delta\epsilon_{OUT}$,were found to be very similar (add order of difference). In this thesis, the average emittance from the two scans, $\epsilon_{avg} = \langle\epsilon_{IN}, \epsilon_{OUT}\rangle$, will be used. The uncertainty on the averaged emittance, $\Delta\epsilon_{avg}$, is computed as:

$$\Delta\epsilon_{avg} = \sqrt{\Delta\epsilon_1^2 + \Delta\epsilon_2^2}, \tag{4.5}$$

where $\Delta\epsilon_1$ is the standard deviation of the ϵ_{IN} and ϵ_{OUT} and $\Delta\epsilon_2 = \sqrt{\langle\Delta\epsilon_{IN}, \Delta\epsilon_{OUT}\rangle}$.

Finally, some emittance increase is expected during each wire scan, due to Coulomb multiple scattering. This effect has been extensivley studied in Ref. [13]. For the rotational SPS WS and the energy of 270 GeV, at which the CC experiments were performed the expected emittance growth from the WS is expected to be small. However, a conservative number of scans were carried, $\sim$ 20 scans per bunch and per plane during $\sim$ 1 hour, in order to minimise the contribution from this effect.

---

dispersion is negligible

4.5   ABWLM

4.6   Wall current monitor

4.7   Conclusions

Post processing steps for the ones I have performed the analysis. The others just menitoned.

5 | Emittance growth measurements with Crab Cavity noise in 2018

In 2018, two prototype Crab Cavities (CCs) were installed in the SPS to be tested for the first time with proton beams. One of the operational issues that needed to be addressed concerned the expected emittance growth due to noise in their RF control system. A theoretical model that describes this emittance growth had already been developed and validated by tracking simulations [1]. Based on those studies a dedicated experiment was performed to benchmark the models with experimental data and to confirm the analytical predictions. In particular, the idea was to inject various noise levels in the CC RF system and record the emittance evolution. In this chapter, the experimental procedure, the measurement methods and results are presented and discussed.

The chapter is stractured as follows: Section 4.2 describes the operational setup for the SPS CC tests and discusses the main diagnostic deployed for the derivation of the CC voltage.

blah blah ... describe sections and subsections after they are completed.

blah blah ... describe sections and subsections after they are completed.

blah blah ... describe sections and subsections after they are completed.

5.1 Crab Cavities in the SPS

For the SPS tests two prototype CCs of the Double Quorter Wave (DQW) type were fabricated by CERN and were assembled into the same cryomodule [2]. The cryomodule was installed in the SPS-LSS6 zone and was placed on a mobile transfer ta-

ble [**GarlaschÃÍ:2648553**]. The table moved with high precision and without breaking the vaccum the cryomodule in the beam line for the CC tests and out of it for the usual SPS operation. For the emittance growth measurements only one of these CCs was used and its main optics and desgin parameters are listed in Table **??**.

5.2 Experimental procedure

5.2.1 Machine and beam configuration

5.2.2 Measurement methods

What do we measure and how? emittance (show plot ws) bunch length ABWLM –> we take the measurement directly from the resposnible tema –> show also from the instrument that we saw the unstable bunches.

5.3 Experimental resutls

5.3.1 Overview

- bunches 2, 3 and 4 unstable

5.3.2 Comparison with the theory

This chapter is adapted from the the studies published in Ref. [14]

5.4 Experimental Setup

Several experimental studies have been performed (2010-2017) to identify the optimal conditions for the emittance growth studies with CCs in the SPS [15, 16]. Based on these preparatory studies, the measurements in the SPS were performed with four low intensity ($\sim 3 \cdot 10^{10}$ ppb) bunches at 270 GeV. To minimise the emittance growth from other sources [16] the first order chromaticity, Q', of the machine was corrected to small positive values ($\sim$ 1-2) in both the horizontal and the vertical planes. During the measurements the Landau octupoles were switched off. It should be note, though, that a residual non-linearity was present in the machine mainly due to multipole components in the dipole magnets [17, 18]. Only one CC was used, providing a vertical kick to the beam. The transverse feedback system was switched off. Even though the emittance growth is a single bunch effect four bunches were used to reduce the statistical uncertainty of the measurements. The distance between the bunhces was 524 ns. An overview of the relevant SPS parameters during the experiment is given in Table

5.4.1 Injected RF noise

In order to characterize the CC noise induced emittance growth, controlled noise was injected into their LLRF system and the evolution of the bunch was recorded for about 20-40 minutes. The injected noise was a mixture of amplitude and phase noise up to 10 KHz, overlapping and primarily exciting the fisrt betatron sideband at $\sim$ 8 kHz. The phase noise was always dominant.

6 | Investigation of the discrepancy

7 | Simple model of describing the decoherence suppression from impedance

8 | Application and impact for HL-LHC

9 | Conclusion

A | Appendix Title

Bibliography

[1] P. Baudrenghien and T. Mastoridis. "Transverse emittance growth due to rf noise in the high-luminosity LHC crab cavities". In: *Phys. Rev. ST Accel. Beams* 18 (10 Oct. 2015), p. 101001. DOI: 10.1103/PhysRevSTAB.18.101001. URL: https://link.aps.org/doi/10.1103/PhysRevSTAB.18.101001.

[2] C. Zanoni et al. "The crab cavities cryomodule for SPS test". In: 874 (July 2017), p. 012092. DOI: 10.1088/1742-6596/874/1/012092. URL: https://doi.org/10.1088/1742-6596/874/1/012092.

[3] Rama Calaga, Ofelia Capatina, and Giovanna Vandoni. "The SPS Tests of the HL-LHC Crab Cavities". In: (2018), TUPAF057. 4 p. DOI: 10.18429/JACoW-IPAC2018-TUPAF057. URL: https://cds.cern.ch/record/2649807.

[4] Rama Calaga. *SPS Crab Cavity test RF Test Program*. Accessed: 11-11-2021. URL: https://indico.cern.ch/event/718127/contributions/2951305/attachments/1645650/2629988/SPSCCtestv3.pdf.

[5] Carver Lee. *First proton beam dynamics results with crab cavities*. Accessed: 10-11-2021. URL: https://indico.cern.ch/event/800428/attachments/1804664/2945632/CrabCavity_BE_Seminar.pdf.

[6] Thomas Levens, Kacper Łasocha, and Thibaut Lefèvre. "Recent Developments for Instability Monitoring at the LHC". In: (2017), THAL02. 4 p. DOI: 10.18429/JACoW-IBIC2016-THAL02. URL: https://cds.cern.ch/record/2313358.

[7] R. Jones and H. Schmickler. "The measurement of Q' and Q" in the CERN-SPS by head-tail phase shift analysis". In: *PACS2001. Proceedings of the 2001 Particle Accelerator Conference (Cat. No.01CH37268)*. Vol. 1. 2001, 531–533 vol.1. DOI: 10.1109/PAC.2001.987561.

A. Bibliography

[8] T. E. Levens et al. "Automatic detection of transverse beam instabilities in the Large Hadron Collider". In: *Phys. Rev. Accel. Beams* 22 (11 Nov. 2019), p. 112803. DOI: 10.1103/PhysRevAccelBeams.22.112803. URL: https://link.aps.org/doi/10.1103/PhysRevAccelBeams.22.112803.

[9] Tom Levens. *Beam instrumentation with SPS Crabs.* Accessed: 11-11-2021. URL: https://indico.cern.ch/event/718127/contributions/2951309/attachments/1646050/2630808/BI_SPS_Crabs.pdf.

[10] Alexander Wu Chao et al. *Handbook of accelerator physics and engineering; 2nd ed.* Singapore: World Scientific, 2013. DOI: 10.1142/8543. URL: https://cds.cern.ch/record/1490001.

[11] J. Bosser et al. "Transverse emittance measurement with a rapid wire scanner at the CERN SPS". In: *Nuclear Instruments and Methods in Physics Research Section A: Accelerators, Spectrometers, Detectors and Associated Equipment* 235.3 (1985), pp. 475–480. ISSN: 0168-9002. DOI: https://doi.org/10.1016/0168-9002(85)90096-8. URL: https://www.sciencedirect.com/science/article/pii/0168900285900968.

[12] OE Berrig et al. *CERN-SPS Wire Scanner Impedance and Wire Heating Studies.* Tech. rep. Geneva: CERN, Sept. 2014. URL: https://cds.cern.ch/record/1972478.

[13] Federico Roncarolo. "Accuracy of the Transverse Emittance Measurements of the CERN Large Hadron Collider". Presented 2005. 2005. URL: https://cds.cern.ch/record/1481835.

[14] Natalia Triantafylou. "INVESTIGATION OF DAMPING EFFECTS OF THE CRAB CAVITY NOISE INDUCED EMITTANCE GROWTH". In: (2021), TBA. DOI: TBA. URL: TBA.

[15] R Calaga et al. "Proton-beam emittance growth in SPS coasts". In: *Conf. Proc.* C1205201 (May 2012), THPPP007. 3 p. URL: https://cds.cern.ch/record/1451286.

[16] Fanouria Antoniou et al. "Emittance Growth in Coast in the SPS at CERN". In: *J. Phys.: Conf. Ser.* 1067 (2018), MOPMF061. 7 p. DOI: 10.18429/JACoW-IPAC2018-MOPMF061. URL: https://cds.cern.ch/record/2649815.

[17]   Michele Carlà et al. "Studies of a New Optics With Intermediate Transition Energy as Alternative for High Intensity LHC Beams in the CERN SPS". In: (2018), TUPAF022. 4 p. DOI: 10.18429/JACoW-IPAC2018-TUPAF022. URL: https://cds.cern.ch/record/2664976.

[18]   Androula Alekou et al. "SPS Long Term Stability Studies in the Presence of Crab Cavities and High Order Multipoles". In: (2018), WEP2PO008. 3 p. DOI: 10.18429/JACoW-HB2018-WEP2PO008. URL: https://cds.cern.ch/record/2640326.